Potential Energy Surface and Vibrational Predissociation Dynamics of $I_2(B)-Ne$

A. García-Vela†

Instituto de Matemáticas y Fısica Fundamental, CSIC, Serrano 123, 28006 Madrid, Spain

Received: March 12, 2002

An empirical potential-energy surface is proposed for the excited B electronic state of the I_2-Ne complex. The potential is represented as an addition of pairwise interactions. The parameters of the potential are fitted to reproduce the main spectroscopic and dynamical data available over a wide range of I_2 vibrational excitations, $v = 13-37$. The experimental information used in the fitting procedure includes the dissociation energy of the complex, resonance decay lifetimes, and I_2 fragment vibrational and rotational distributions. The simulations of the complex vibrational predissociation dynamics required to fit the potential parameters are carried out by means of an exact wave packet method. The fitted potential surface reproduces the available data typically within experimental error, which assesses its reliability, at least in the range of vibrational excitations studied. The predissociation dynamics of $I_2(B,v)-Ne$ is discussed in light of the results.

I. Introduction

Weakly bound van der Waals (vdW) $BC-Rg_n$ complexes (BC = diatomic molecule, Rg = rare gas atom) are prototype systems to explore unimolecular dissociation and energy transfer processes. Upon optical excitation of the diatomic subunit, part of the energy initially deposited is transferred to the intermolecular modes, leading to fragmentation of the complex. Among such energy transfer processes are electronic, vibrational, and rotational predissociation, internal vibrational redistribution, and evaporative cooling.

The dissociation dynamics of a large variety of vdW complexes has been the subjet of experimental investigation.[1−12] The smallest, triatomic BC−Rg complexes were those most extensively studied, due to their relative simplicity. Among them, the vibrational predissociation (VP) dynamics of the I_2-Ne complex in the excited B electronic state has been explored by several experimental groups. Levy and co-workers studied the VP of $I_2(B,v)-Ne$ for low ($v = 9-14$)[1] and high ($v = 32-34$)[4] initial vibrational excitations of I_2, and they reported the first estimate of the $I_2(B)-Ne$ dissociation energy,[4] $65 < D_0 < 67$ cm^{-1}. Zewail and co-workers carried out real-time experiments[9] on the VP process $I_2(B,v)-Ne \rightarrow I_2(B,v-1) + Ne$ and extracted complex decay lifetimes in the range $v = 13-23$. More recently, Heaven and co-workers have probed the predissociation dynamics of $I_2(B,v)-Ne$ in the range $v = 29-41$, and they found a new estimate of the $I_2(B,v=34)-Ne$ dissociation energy,[12] $D_0 = 57.6 \pm 1.0$ cm^{-1}, lower than that of Levy and co-workers.[4] All the above experimental data provide spectroscopic and dynamical information on the $I_2(B)-Ne$ complex over a wide range of diatomic vibrational excitations.

On the theoretical side, studies on the VP dynamics of I_2-Ne include collinear geometry calculations applying the distorted-wave Born approximation,[13] quasiclassical trajectory calculations,[14−16] and approximate full-dimensional quantum simulations based on the time-dependent self-consistent-field (TDSCF) approach.[17] One of the difficulties in the theoretical treatment of the I_2-Ne predissociation dynamics arises from the absence of accurate ab initio potential-energy surfaces. In general, ab initio calculations on vdW complexes containing I_2 are not straightforward, due to the large number of electrons involved and to relativistic effects. The excited character of the B electronic state poses an additional difficulty.[18] At present no ab initio potentials are available for either the ground X or the excited B electronic state of I_2-Ne. A semiempirical potential based on the diatomic-in-molecules approximation[16] has been proposed for $I_2(B)-Ne$. Empirical potentials have been commonly used in dynamical calculations.[15−17] Such potentials are typically represented as a sum of pairwise interactions, the parameters of which are fitted to reproduce the available spectroscopic and dynamical data.[15]

The empirical potential[15] used in some of the latest simulations of the $I_2(B)-Ne$ VP[15,17] was fitted with an approximate quantum model, to reproduce the I_2-Ne dissociation energy estimated by Levy and co-workers,[4] and the decay lifetimes reported by Zewail and co-workers.[9] The recent experiments of Heaven and co-workers[12] provide additional information, and suggest that the above empirical potential should be refined. The main goal of this paper is to characterize an empirical potential surface for $I_2(B)-Ne$ consistent with the experimental data available at present. To this purpose the resonance states of $I_2(B,v)-Ne$ have been calculated variationally in the range $v = 13-37$ to fit the potential according to the spectroscopic data. Then the VP dynamics of these resonance states is simulated with an exact full-dimensional wave packet method to fit the potential to reproduce the dynamical data. Once the empirical potential is characterized, the dissociation dynamics are analyzed over the whole range of vibrational excitations studied. To the best of the author's knowledge these are the first exact calculations on the $I_2(B,v)-Ne$ VP dynamics.

The organization of the paper is the following. In section II the methodology used to characterize the potential, and the resonance state and dynamical calculations are described in detail. Results are presented and discussed in section III. Finally, conclusions are given in section IV.

II. Theory

A. Potential-Energy Surface. The potential-energy surface of the B electronic state of I_2-Ne is represented as a sum of atom−atom interactions

† E-mail: garciavela@imaff.cfmac.csic.es.

10.1021/jp020690o CCC: $22.00
Published on Web 06/25/2002

$$V = V_{I_a-I_b} + V_{I_a-Ne} + V_{I_b-Ne} \quad (1)$$

The analytical form reported in ref 19 has been used for the V_{I-I} interaction potential.[20] This potential was inverted from ultrafast laser experiments. Regarding each I−Ne interaction, a Morse functional form is assumed,

$$V_{I-Ne}(d) = D[e^{-2\alpha(d-d_e)} - 2e^{-\alpha(d-d_e)}] \quad (2)$$

Thus the fit of the $I_2(B)-Ne$ potential surface involves only fitting the Morse parameters D, α, and d_e of the I−Ne interaction potential. Actually, the same I−Ne equilibrium distance as that of the empirical potential of ref 15, $d_e = 4.36$ Å, has been used in this work. Therefore the fitting procedure reduces to the D and α parameters of eq 2.

The representation of the $I_2(B)-Ne$ potential surface of eqs 1 and 2 has two advantages for theoretical simulations. One is that it is easy to implement and computationally efficient. The other advantage is that it is straightforward to extend this representation for larger clusters I_2-Ne_n ($n > 1$), just by adding the Ne−Ne interaction potential.[21]

The following experimental information has been used as a criterion to fit the parameters of eq 2. The potential is required to predict a $I_2(B,v=34)-Ne$ dissociation energy $D_0 = 57.6$ cm^{-1}, and that the $\Delta v = -1$ predissociation channel is energetically closed for $v > 36$, as found by Heaven and co-workers.[12] The potential is also required to reproduce the decay lifetimes reported by Zewail and co-workers[9] for $v = 13-23$ within the experimental error bars or close to their limits. Decay lifetimes were not reported in ref 12 for high vibrational excitations. However, other dynamical information reported by Heaven and co-workers[12] has been used to assess the validity of the fitted potential. This includes the gradual suppression of the $\Delta v = -1$ decay channel in the range $33 \leq v \leq 36$ (also observed by Levy and co-workers[4]), and the highest rotational levels of the I_2 fragment populated through the $\Delta v = -1$ and $\Delta v = -2$ predissociation channels.

B. Calculation of the $I_2(B,v)-Ne$ Resonance States. As pointed out above, one of the requirements of the potential is to reproduce the experimental dissociation energy $D_0 = 57.6$ cm^{-1} for $I_2(B,v=34)-Ne$. The dissociation energy of $I_2(B,v)-Ne$ coincides with the energy of the ground resonance state of the complex in the vibrational level v. Therefore the parameters of the I−Ne potential are varied until the ground resonance energy of $I_2(B,v=34)-Ne$ matches the required value for the dissociation energy. To simulate the VP dynamics, in addition to the resonance energy the ground resonance wave function must be calculated to be used as the initial state of the system. In the following the method employed to calculate the resonance states of $I_2(B,v)-Ne$ for the vibrational excitations $v = 13-23$, 26, 29, 32−37 studied, is described.

The I_2-Ne system is represented in Jacobian coordinates (r, R, θ), where r is the I−I distance, R is the separation between the Ne atom and the center-of-mass of I_2, and θ is the angle between the vectors associated with the r and R coordinates. Zero total angular momentum is assumed in the calculations. To calculate the resonance states of $I_2(B,v)-Ne$, the I_2 stretching vibration is separated within the vibrational diabatic approximation.[22] In this approximation the resonance wave function is expressed as the product

$$\Phi(r,R,\theta) = \chi_v(r)\, \varphi^{(v)}(R,\theta) \quad (3)$$

where $\chi_v(r)$ is a vibrational eigenstate of the $I_2(B)$ diatomic molecule, and the vdW wave function $\varphi^{(v)}(R,\theta)$ is obtained variationally by diagonalizing the vibrationally averaged Hamiltonian $\hat{H}_{vv} = \langle \chi_v(r)|\hat{H}|\chi_v(r)\rangle$, once it is represented on a suitable basis set ($\hat{H}$ is the full Hamiltonian of $I_2(B)-Ne$). The above approximation is justified because of the frequency difference between the I_2 vibration and the vdW modes. As it has been discussed,[23] the vibrational mixing of the χ_v states is quite small for this type of systems. Thus, the present resonance states, which are actually zero-order ones, resemble very closely the true resonance states of the complex.

C. Vibrational Predissociation Dynamics. The decay dynamics of the ground resonance state, $I_2(B,v)-Ne \rightarrow I_2(B,v_f<v) + Ne$ is simulated by solving the time-dependent Schrödinger equation for the wave packet $\Phi(r,R,\theta,t)$. To this purpose the r and θ dependence of $\Phi(r,R,\theta,t)$ is expanded on a basis set consisting of the $\chi_v(r)$ vibrational states and the $P_j(\theta)$ Legendre polynomials, respectively.[23] The coefficients of the expansion, $C_{v,j}(R,t)$, are represented on a grid, and they are the packets that are actually propagated. The wave packet is absorbed before it reaches the edges of the grid in the R coordinate. Absorption is carried out after each propagation time step by multiplying each packet $C_{v,j}(R,t)$ by the function $\exp[-\alpha(R - R_{abs})^2]$, for $R > R_{abs}$, with $\alpha = 0.04$ au^{-2} and $R_{abs} = 25.0$ au.

Resonance lifetimes can be extracted from the time evolution of the square of the wave packet autocorrelation function $P(t) = |\langle\Phi(0)|\Phi(t)\rangle|^2$. By fitting the decay curve $P(t)$ to an exponential law $P(t) \simeq e^{-t/\tau}$ [or equivalently, by fitting $\ln P(t)$ to the straight line $-t/\tau$], the resonance lifetime τ is obtained.[17,23] It has been shown[24] that by propagating the wave packet until a final time t_f, one can obtain the autocorrelation function until a time $2t_f$. However, to take advantage of this feature of the autocorrelation function poses some difficulties due to the absorption of the wave packet.[25] To calculate the autocorrelation function until a time $2t_f$, the procedure described in ref 25 has been adopted here.

In addition to resonance lifetimes, vibrational and rotational distributions of the I_2 product fragment have also been computed. The probability $P_{v_f}(t)$ of $I_2(B,v_f)$ fragments in $v_f = v - 1$, $v - 2$, ..., is calculated by accumulating probability in the region of the products $I_2(B,v_f) + Ne$, $R > R_c$ (including the absorption region), in which the vdW bond can be considered broken.[25,27,28]

In a typical finite time propagation, at final time t_f there is wave packet intensity in the interaction region corresponding to complexes that still did not dissociate to $I_2 + Ne$. As a consequence, the absolute probabilities $P_{v_f}(t_f)$ calculated as indicated above are not indicative of the final values $P_{v_f}(t\rightarrow\infty)$, unless that very long and costly propagations are carried out. As discussed previously,[25,28] reliable estimates of the final vibrational populations can be obtained without the need of long propagations, by monitoring the time evolution of the relative or normalized probabilities

$$P^{norm}_{v_f}(t) = \frac{P_{v_f}(t)}{\sum_v P_v(t)} \quad (4)$$

In BC−Rg complexes the form of the product distributions is essentially determined by the short-time dynamics.[25,28] Thus, if enough time is allowed (typically a few picoseconds) for all the dissociation mechanisms contributing with probability to a given final vibrational channel v_f to be operating, the probabilities $P^{norm}_{v_f}(t)$ converge to constant values. Such values provide good estimates for the final vibrational populations of the $I_2(B,v_f)$ fragment.

TABLE 1: Morse Parameters of the Present and Previous[15] I−Ne Interaction Potentials

	D (cm^{-1})	α (Å^{-1})	d_e (Å)
present potential	38.03	1.596	4.36
previous potential	40.75	1.56	4.36

Rotational distributions of the $I_2(B,v_f,j_f)$ fragment are calculated as the asymptotic $t \rightarrow \infty$ limit of

$$P_{v_f j_f}(E,t) = \left| \int_{R_a}^{R_b} \left(\frac{\mu_{I_2-Ne}}{2\pi k_{v_f j_f} \hbar^2} \right)^{1/2} e^{-ikv_f j_f R} C_{v_f j_f}(R,t)\, dR \right|^2 \quad (5)$$

where $k_{v_f,j_f} = [2\mu_{I_2-Ne}(E - E_{v_f,j_f})]^{1/2}$ and $E_{v_f,j_f} = E_{v_f} + j_f(j_f + 1)\langle\chi_{v_f}(r)|r^{-2}|\chi_{v_f}(r)\rangle/2\mu_{I_2}$. The energy E is taken to be the mean energy of the system, which is very close to the resonance energy.

D. Computational Details. The $C_{v,j}(R,t)$ packets were represented on a uniform grid in the R coordinate, with the grid parameters $R_0 = 5.0$ au, $\Delta R = 0.25$ au, and the number of grid points $N_R = 128$. In the basis set expansion of $\Phi(r,R,\theta,t)$ four vibrational functions $\chi_v(r)$, corresponding to $v = v$, $v - 1$, $v - 2$, $v - 3$, and 45 (even) rotational states ($j_{max} = 88$) were used for the dynamical calculations in the range $v = 13-23$ of I_2 vibrational excitations. For $v = 26$, 29, 32−37 five vibrational states ($v = v$, $v - 1$, $v - 2$, $v - 3$, $v - 4$) and 56 (even) rotational states ($j_{max} = 110$) were used to expand the wave packet. The time propagation of the $C_{v,j}(R,t)$ packets was carried out by means of the Chebychev polynomial expansion method,[26] with a time step $\Delta t = 0.01$ ps. The Hamiltonian operations on $C_{v,j}(R,t)$ involving kinetic-energy terms were performed using fast Fourier transform (FFT) techniques. The time propagation was carried out until a final time $t_f = 15$ ps for $v = 22$, 23, 26, 29, 32−37. The propagation time was gradually increased as v decreases up to $t_f = 35$ ps for $v = 13$. For the analysis of I_2 product vibrational distributions it is considered that for distances $R > R_c = 20$ au the vdW bond is effectively broken. The I_2 rotational distributions are calculated in the region limited by $R_a = 20$ au and $R_b = 25$ au.

III. Results and Discussion

The parameters of the I−Ne interaction potential fitted according to the experimental data are listed in Table 1. The parameters of the previous empirical I−Ne potential[15] are also collected in the table for the sake of comparison. In the following the predictions of the present I_2(B)−Ne potential regarding resonance energies, decay lifetimes, and I_2 product distributions are presented and compared to the available data.

A. Resonance Energies. Ground resonance energies of the $I_2(B,v)$−Ne complex were calculated for the vibrational excitations $v = 13-23$, 26, 29, 32−37, and they are listed in Table 2 along with the I_2 vibrational energy levels E_v. The present potential yields a dissociation energy of 57.6 cm^{-1} for I_2-(B,v=34)−Ne, as found experimentally,[12] and similar dissociation energies for the complex in the range $32 \leq v \leq 37$. The potential also predicts that the $\Delta v = -1$ predissociation channel is energetically closed for $v = 37$ (by 0.5 cm^{-1}), in agreement with the experimental result of Heaven and co-workers.[12] Thus the proposed potential takes into account the main energetic features observed experimentally.[12]

With the previous empirical potential[15] the dissociation energy calculated for I_2(B,v=34)−Ne is 62.72 cm^{-1}. This potential predicts ground resonance energies for the different I_2 vibrational levels that are about 5 cm^{-1} lower than those of Table 2, since the well depth of the I−Ne interaction is 2.7 cm^{-1} larger (see Table 1). As a result, the $\Delta v = -1$ channel is nearly closed energetically for $v = 34$, in agreement with the experimental finding of Levy and co-workers.[4] The changes in the present potential parameters are not large as compared with the previous parameters, consistent with the fact that the $I_2(B,v)$−Ne dissociation energies estimated by Heaven and co-workers and Levy and co-workers differ by a few cm^{-1}. However, such changes in the potential surface will have an increasingly important effect when larger $I_2(B)-Ne_n$ clusters are modeled as n increases.

TABLE 2: Calculated Ground Resonance Energies of $I_2(B,v)$−Ne Relative to the Initial I_2 Vibrational Energy Level E_v

v	E_{res} (cm^{-1})	E_v[a] (cm^{-1})
13	−58.73	−2827.47
14	−58.70	−2724.97
15	−58.66	−2624.32
16	−58.62	−2525.54
17	−58.59	−2428.64
18	−58.54	−2333.64
19	−58.50	−2240.56
20	−58.46	−2149.42
21	−58.41	−2060.22
22	−58.37	−1972.99
23	−58.32	−1887.73
26	−58.16	−1643.94
29	−57.97	−1418.31
32	−57.76	−1211.02
33	−57.68	−1146.01
34	−57.60	−1083.05
35	−57.51	−1022.14
36	−57.42	−963.27
37	−57.32	−906.44

[a] $E_v = 0$ corresponds to separated atoms.

TABLE 3: Calculated and Experimental (with Error Bars) Resonance Decay Lifetimes

v	τ (ps)	τ^{exp} (ps)[a]
13	257.5	216 ± 16
14	216.5	196 ± 12
15	177.0	182 ± 20
16	150.7	160 ± 15
17	129.1	126 ± 12
18	110.2	107 ± 9
19	89.5	87 ± 4
20	76.3	78 ± 4
21	68.2	69 ± 6
22	56.7	58 ± 3
23	46.0	53 ± 3
26	28.4	
29	16.8	
32	12.1	
33	8.9	
34	8.6	
35	7.1	
36	6.8	
37	5.5	

[a] Reference 9.

B. Resonance Decay Lifetimes. The vibrational predissociation dynamics is simulated for all the ground resonance states listed in Table 2, and decay lifetimes are obtained as described in section II.C. They are collected in Table 3 (second column) along with the lifetimes reported by Zewail and co-workers from real-time experiments[9] for $v = 13-23$ (third column). For a better comparison the calculated and experimental lifetimes are also plotted in Figure 1.

For most of the I_2 vibrational excitations the τ lifetimes predicted by the present potential are within the experimental error bars, or close to their limits. In general, the values of τ

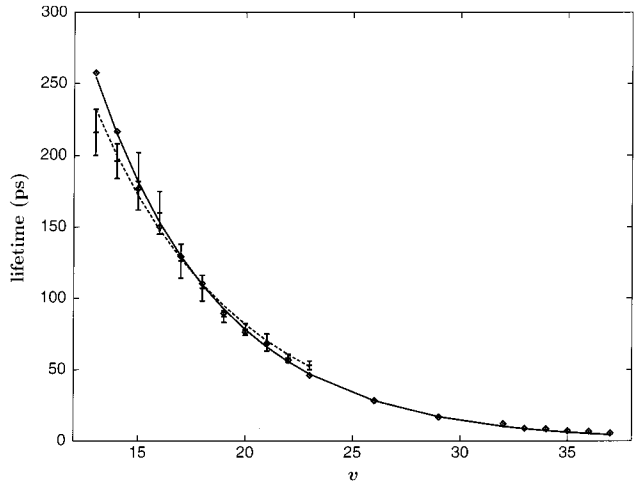

Figure 1. Plot of the calculated τ ($\diamond$) and experimental (with error bars) resonance lifetimes presented in Table 3 vs the initial I_2 vibrational excitation v. Exponential fits (eq 6) of the calculated (solid line) and experimental (dashed line) lifetimes are also shown.

deviate from the experimental ones by less than 6.3% (and typically around 1−3%). Only for $v = 13$, $v = 14$, and $v = 23$ are the deviations of τ larger, 19.2%, 10.5%, and 13.2%, respectively. Reducing the deviations of τ for $v = 13$ and $v = 14$ (by changing the potential parameters) implies an increase of the deviations of τ for higher v, particularly for $v = 23$. When the potential parameters are fitted, the criterion followed here has been to reproduce better the experimental lifetimes with smaller error bars, i.e., those for $v = 19-23$.

For BC−Rg complexes a nonlinear decrease of the VP lifetime (or equivalently, a nonlinear increase of the predissociation rate $k = \tau^{-1}$) with increasing v is typically found. Such a nonlinear behavior of $\tau(v)$ has been rationalized in terms of the energy gap law[22] and the anharmonicity of the BC potential. Following this law, as the energy difference between the initial and the final levels v and v_f of BC matches the dissociation energy of the BC−Rg complex (i.e., the kinetic energy available for the Rg fragment $\epsilon \rightarrow 0$), the predissociation lifetime decreases. The VP lifetime depends mainly on the couplings between the initial resonance of the complex and the continuum states to which it decays. Such couplings increase (and therefore τ decreases) as the continuum states become less oscillating, i.e., when ϵ decreases. Due to the anharmonicity of the BC potential, as v increases, the energy available for the predissociation fragments (and therefore ϵ) decreases, which explains the decrease of τ with increasing v. The specific shape of the $\tau(v)$ curve (e.g., exponential, $1/v^2$, etc.) is determined by the specific couplings associated with the BC−Rg potential surface.

The lifetimes calculated for I_2(B)−Ne exhibit a nonlinear behavior with v, in agreement with the experimental findings.[9] The authors of ref 9 fitted the behavior of the predissociation rate k with v to several analytical forms. One of the best fits was to an exponential law, $\tau^{-1} \propto e^{\gamma v}$, with $\gamma = 0.1493$. In Figure 1 a similar fit of the experimental lifetimes to the curve

$$\tau = Ae^{-\gamma v} \tag{6}$$

with $A = 1615.88$ ps and $\gamma = 0.1493$ is reproduced (dashed line). The calculated lifetimes also fit remarkably well to the exponential law of eq 6 with $A = 2290.0$ ps and $\gamma = 0.169$ (solid line of Figure 1), over the whole range of v investigated. The two exponential curves of Figure 1 are very close for $v \geq 18$, and gradually deviate for $v < 18$ due to the larger deviations of the calculated lifetimes from the experimental ones for $v = 13$, 14. Despite these deviations the agreement between the curves is in general quite good, as a result of the good agreement between the experimental and calculated lifetimes. Thus the present I_2(B)−Ne potential surface predicts a nonlinear, specifically exponential behavior of the resonance decay lifetime with the vibrational excitation, over the range $v = 13-37$ studied. Such a behavior agrees with that found experimentally[9] for $v = 13-23$ excitations.

TABLE 4: Calculated I_2 Fragment Vibrational State Distributions (in Percentage) for the Dissociation Channels $v - 1$, $v - 2$, $v - 3$, and $v - 4$

v	$v-1$	$v-2$	$v-3$	$v-4$
13	97.1	2.8	0.1	
14	96.7	3.2	0.1	
15	96.3	3.6	0.1	
16	95.8	4.0	0.2	
17	95.3	4.5	0.2	
18	94.6	5.2	0.2	
19	93.9	5.8	0.3	
20	93.3	6.3	0.4	
21	92.5	7.1	0.4	
22	91.2	8.2	0.6	
23	90.3	9.1	0.6	
26	85.2	12.9	1.7	0.2
29	78.4	18.2	3.0	0.4
32	69.0	25.0	5.3	0.7
33	60.8	30.9	7.2	1.1
34	53.2	36.1	9.3	1.4
35	41.9	43.0	12.8	2.3
36	26.0	54.2	16.7	3.1
37	8.7	64.8	22.0	4.5

It should be noted that the experimental lifetime for $v = 13$ is noticeably lower than the value predicted by the exponential fit of Zewail and co-workers,[9] which coincides with the upper limit of the error bar. It might happen that the simple exponential form that seems to be valid to describe the behavior of the lifetime for $v > 13$, begins to be no longer valid for $v \leq 13$. Experimental data of the complex decay lifetime for $v < 13$ would be required to discern this question.

C. I_2 Product Fragment Distributions. Vibrational populations of the $I_2(B,v_f)$ fragment produced after VP are listed in Table 4 for all the v excitations studied. As seen from the table, the present potential predicts that $I_2(B,v)$−Ne VP occurs dominantly through the $\Delta v = -1$ channel in the range $13 \leq v \leq 34$, and particularly for the vibrational excitations $v = 13-23$, for which the $v - 1$ population is >90%. For $v \geq 35$ the dominant predissociation channel is $\Delta v = -2$.

Rapid suppression of the $\Delta v = -1$ decay channel is predicted by the proposed $I_2(B,v)$−Ne potential for $v > 32$, in agreement with the experimental findings.[12] It is stressed that in the present dynamical calculations dissociation of the I_2(B)−Ne complex occurs only via vibrational predissociation. The implication is that suppression of the $\Delta v = -1$ predissociation channel is only due to the vibrational predissociation dynamics occurring in the B electronic state, without the need to invoke the influence of electronic predissociation. The above interpretation of the partial suppression of the $\Delta v = -1$ channel for high I_2 vibrational excitations was suggested by Heaven and co-workers,[12] and the theoretical results of Table 4 come to confirm it.

Actually the weight of the $\Delta v = -1$ channel decreases gradually over the whole range $13 \leq v \leq 37$ investigated, although this decrease is faster for $v > 32$. A plausible explanation is that as v increases and the I_2 vibrational energy levels become closer, potential couplings responsible for the $\Delta v \leq -2$ decay channels become increasingly intense. Thus, gradual suppression of the $\Delta v = -1$ channel would be caused by the competition of the $\Delta v \leq -2$ predissociation channels.

This interpretation seems to be supported by the fast increase for $v > 32$ not only of the $v-2$ population, but also of the $v-3$ and $v-4$ populations. In this sense it is remarkable the relatively high populations of the $I_2(B,v_f=v-3)$ and $I_2(B,v_f=v-4)$ fragments found in the present calculations for $v \geq 33$.

It is apparently surprising that despite that the $\Delta v = -1$ channel is energetically closed for $v = 37$ (see Table 2), a 8.7% of $v-1$ population is found in the calculations. The reason is that the initial resonance wave packet has a dispersion in energy. Indeed, from the lifetimes τ of Table 3, one can calculate the fwhm of the resonance level as $\Gamma = \hbar/\tau$. This resonance width ranges from $\Gamma = 0.44$ cm^{-1} for $v = 32$ up to $\Gamma = 0.97$ cm^{-1} for $v = 37$. Therefore the ground resonance width for $v = 37$ is twice the 0.5 cm^{-1} by which the $\Delta v = -1$ channel is energetically closed, and the 8.7% of $I_2(B,v_f=v-1)$ population comes from wave packet components associated with energies > -56.83 cm^{-1}, for which the $\Delta v = -1$ channel is energetically open. When energy-resolved $P_{v_f j_f}(E,t_f)$ distributions are calculated through eq 5, the results are $P_{v_f=36,j_f}(E,t_f) = 0$ for all j_f, and therefore $P^{\text{norm}}_{v_f=36}(E,t_f) = \sum_{j_f} P^{\text{norm}}_{v_f=36,j_f}(E,t_f) = 0$ in the range of energies E ($\sim$0.5 cm^{-1}) where the $\Delta v = -1$ channel is closed. The energy resolution of the spectra from which the I_2 vibrational distributions were obtained was of 0.3 cm^{-1} line width.[12] With this spectral resolution Heaven and co-workers[12] found no population of the $I_2(B,v_f=36)$ fragment, and from this absence they concluded that the $\Delta v = -1$ channel is closed for $v = 37$. Thus, the theoretical result of zero $I_2(B,v_f=36)$ population for energies E up to 0.5 cm^{-1} higher than the $v = 37$ resonance energy is consistent with the experimental absence of $I_2(B,v_f=36)$ population when $I_2(B,v=37)-Ne$ energies higher than the resonance energy up to 0.15 cm^{-1} (half the spectral resolution line width) are probed.

In the experiments of Heaven and co-workers[12] it was found that the $\Delta v = -1$ decay channel is dominant for $v < 33$. With the present potential surface the $\Delta v = -1$ channel is dominant for $v < 35$, as seen from the results of Table 4. One possible reason of this slight discrepancy is that the potential surface overestimates to some extent the weight of the $\Delta v = -1$ channel in the VP dynamics. Small differences in the conditions at which the dynamics takes place between the experiments and the calculations (e.g., in the system temperature and the theoretical characterization of the initial resonance state) could also be partially responsible for this disagreement.

Rotational distributions of the $I_2(B,v_f,j_f)$ fragment have been calculated for the predissociation channels $v_f = v-1$ and $v_f = v-2$, and they are shown in Figure 2 for several initial v excitations over the range studied. The distributions correspond to the even rotational states j_f. Since I_2 is a homonuclear molecule, only either the even or the odd rotational states need to be included in the calculation, and the even states have been chosen here.

It should be noted that the present distributions differ from those previously calculated with the approximate quantum TDSCF method.[17] The TDSCF calculations predicted much colder rotational distributions than the exact ones of Figure 2 (for a comparison see the TDSCF distributions associated with the $\Delta v = -1$ channel for $v = 19$, 21, 23 in Figure 8 of ref 17). As discussed previously,[29] the TDSCF model underestimates energy transfer to the bending mode when it is explicitly factorized in the total wave function (as done in the calculations of ref 17), leading to less rotational excitation of the $I_2(B)$ fragment.

The present I_2 rotational distributions found for the $\Delta v = -1$ channel are rather cold, with most of the population

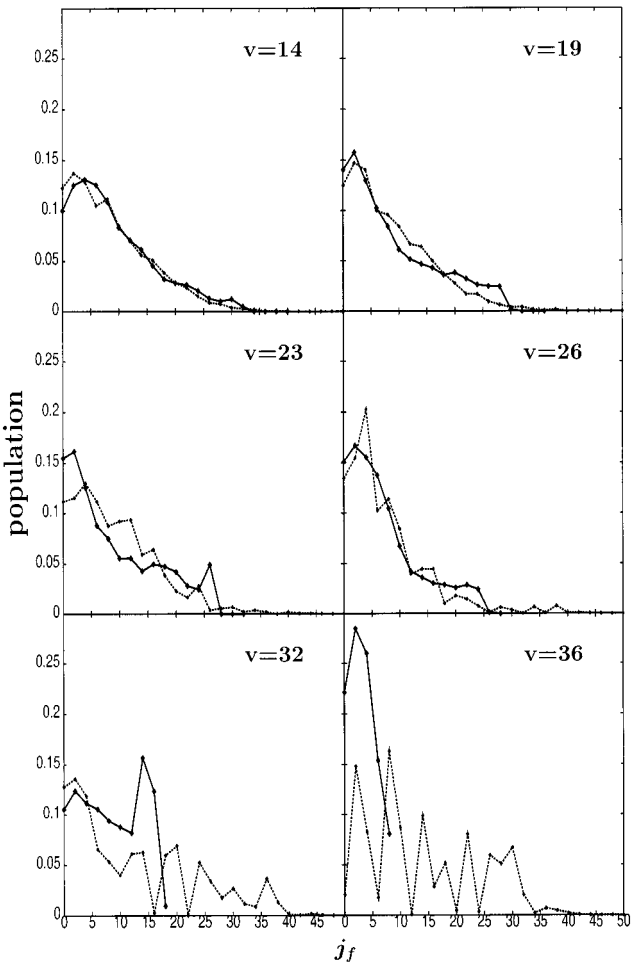

Figure 2. Calculated rotational distributions of the $I_2(B,v_f)$ fragment produced after predissociation of the complex through the $v_f = v-1$ (solid lines) and $v_f = v-2$ (dashed lines) channels for several vibrational excitations v. All the distributions are normalized to unity.

concentrated at low j_f states. As v increases in the range $v = 13-37$ studied, the highest rotational state populated with appreciable intensity, $j_f^{\max}$, decreases, consistent with the fact that the energy available for dissociation through the $\Delta v = -1$ channel, $E_v - E_{v-1}$, decreases with increasing v (see Table 2). For $v \leq 23$ $j_f^{\max}$ is lower than the highest rotational state energetically open, but as v increases, particularly for $v \geq 32$, the rotational channels become gradually closed. The closing of the rotational channels is likely to be related to the suppression of the $\Delta v = -1$ predissociation channel. In the case of $v = 32$, $j_f^{\max} = 18$ coincides with the highest rotational channel energetically open. This result is in good agreement with the experimental detection of $j_f^{\max} = 17$ for the $\Delta v = -1$ channel of $v = 32$. In general the rotational distributions exhibit little structure. These cold and rather unstructured rotational distributions are consistent with fragmentation of the complex via direct predissociation through the $\Delta v = -1$ channel, as found experimentally[12] as well.

The rotational distributions associated with the $\Delta v = -2$ predissociation channel (Figures 2 and 3) are also relatively cold (particularly for $v \leq 26$) and extend up to values of $j_f^{\max}$ remarkably lower than the highest one energetically accessible. From Figures 2 and 3 it is found that $j_f^{\max} = 44$ for $v = 32$ and $v = 33$, and $j_f^{\max} = 40$ for $v = 35$. These results agree quite well with the experimental findings that $j_f^{\max} = 43$ for $v = 32$ and $j_f^{\max} = 42$ for $v = 33$ and $v = 35$. The rotational distributions are essentially unstructured for $v \leq 22$. For higher

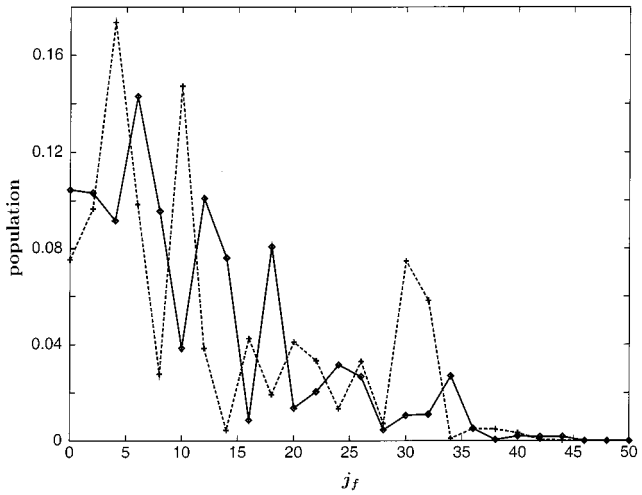

Figure 3. Calculated rotational distributions of the $I_2(B,v-2)$ fragment after predissociation of $I_2(B,v)-Ne$ from $v = 33$ (solid line) and $v = 35$ (dashed line). The two distributions are normalized to unity.

vibrational excitations the $\Delta v = -2$ distributions gradually develop a structure. Interestingly, for $v \geq 32$ the rotational distributions become increasingly hotter and they exhibit a pronounced structure.

The rotational structure predicted by the present potential for $v \geq 32$ seems to indicate that for high vibrational excitations the initial resonance is more strongly coupled to some continuum states, associated with specific rotational states and energies ϵ of the $I_2(B,v_f=v-2,j_f)$ and Ne fragments, respectively. The higher rotational excitation found for $v \geq 32$ is also consistent with this possibiltiy, due to the energy gap law. As the energy available for the fragments, $E_v - E_{v-2}$, decreases with increasing v, rotational excitation seems to be favored since it implies smaller ϵ energies, and therefore a stronger coupling to the corresponding continuum states.

IV. Summary and Conclusions

The vibrational predissociation dynamics of $I_2(B,v)-Ne$ is simulated with an exact wave packet method over the range $v = 13-37$. On the basis of these simulations an empirical potential surface for the I_2-Ne complex in the excited B electronic state is fitted. The potential is represented as a sum of atom−atom interactions. The parameters of the potential surface are fitted to reproduce the main spectroscopic and dynamical data available. Among the spectroscopic information used to fit the potential is the recent estimate of the dissociation energy of the $I_2(B,v=34)-Ne$ complex, $D_0 = 57.6 \pm 1$ cm^{-1}, and the finding that the $\Delta v = -1$ predissociation channel closes for $v > 36$.[12] The dynamical information involves predissociation lifetimes in the range $v = 13-23$ of I_2 vibrational excitations.[9] Additional dynamical information on I_2 fragment vibrational and rotational distributions reported for high v excitations[12] is also used to assess the validity of the potential surface proposed.

The present potential reproduces a dissociation energy of 57.6 cm^{-1} for $I_2(B,v=34)-Ne$ and shows that the $\Delta v = -1$ predissociation channel is energetically closed for $v > 36$, in agreement with the experimental observations.[12] The calculated predissociation lifetimes in the range $v = 13-23$ reproduce the experimental ones within the reported error bars[9] or very close to their limits. Differences between the experimental lifetimes and those predicted by the fitted potential are typically <6.3%. The present lifetimes exhibit an exponential behavior with the I_2 vibrational excitation in the whole range of v investigated.

The potential surface predicts the partial suppression of the $\Delta v = -1$ channel for $v > 32$, in accordance with the experimental finding.[12] This result confirms the previous interpretation of Heaven and co-workers based on their observations,[12] that such a suppression is due to the vibrational predissociation dynamics, and not to electronic predissociation. It is suggested, in light of the present results, that the suppression of the $\Delta v = -1$ channel could be due to an increase of the intensity of the potential couplings responsible for the $\Delta v \leq -2$ decay channels as v increases. The gradual closing of rotational channels found for $v \geq 32$ could also contribute to the suppression of the $\Delta v = -1$ predissociation channel. The calculated I_2 rotational distributions for the $\Delta v = -1$, -2 predissociation channels are found to be rather cold and essentially unstructured in general, particularly for $v < 23$. In the distributions of the $\Delta v = -2$ channel an increasing structure and rotational excitation appears for $v > 23$, and in particular for $v \geq 32$. This would indicate a stronger coupling of the initial resonance state with specific continuum states, for high v excitations. The highest I_2 rotational state populated predicted by the calculations agrees well with the experimental values reported for $v \geq 32$. The present rotational distributions are consistent with fragmentation of the complex via direct predissociation, which is supported by the experimental evidence.[12]

The empirical potential surface proposed for $I_2(B,v)-Ne$ reproduces the main spectroscopic and dynamical observations, typically within experimental error, over a wide range of v excitations. In addition, the simplicity of its representation makes the present potential surface very efficient to be used in dynamical simulations. In this sense, it is viewed as a reliable and efficient potential to model larger I_2-Ne_n ($n > 1$) complexes, to simulate the vibrational predissociation dynamics.

Acknowledgment. This work was supported by CICYT, Spain, Grant No. BFM-2001-2179, and by the EU network TMR Grant No. HPRN-CT-1999-00005.

References and Notes

(1) Kubiak, G.; Fitch, P. S. H.; Wharton, L.; Levy, D. H. *J. Chem. Phys.* **1978**, *68*, 4477.

(2) Sharfin, W.; Johnson, K. E.; Wharton, L.; Levy, D. H. *J. Chem. Phys.* **1979**, *71*, 1292.

(3) Kenny, J. E.; Johnson, K. E.; Sharfin, W.; Levy, D. H. *J. Chem. Phys.* **1980**, *72*, 1109.

(4) Blazy, J. A.; DeKoven, B. M.; Russell, T. D.; Levy, D. H. *J. Chem. Phys.* **1980**, *72*, 2439.

(5) Swartz, B. A.; Brinza, D. E.; Western, C. M.; Janda, K. C. *J. Phys. Chem.* **1984**, *88*, 6272.

(6) Drobits, J. C.; Lester, M. I. *J. Chem. Phys.* **1987**, *86*, 1662.

(7) Hair, S. R.; Cline, J. I.; Bieler, C. R.; Janda, K. C. *J. Chem. Phys.* **1989**, *90*, 2935.

(8) Evard, D. D.; Bieler, C. R.; Cline, J. I.; Sivakumar, N.; Janda, K. C. *J. Chem. Phys.* **1988**, *89*, 2829.

(9) Willberg, D. M.; Gutmann, M.; Breen, J. J.; Zewail, A. H. *J. Chem. Phys.* **1992**, *96*, 198. Gutmann, M.; Willberg, D. M.; Zewail, A. H. *J. Chem. Phys.* **1992**, *97*, 8037.

(10) Gutmann, M.; Willberg, D. M.; Zewail, A. H. *J. Chem. Phys.* **1992**, *97*, 8048.

(11) Burroughs, A.; Heaven, M. C. *J. Chem. Phys.* **2001**, *114*, 7027.

(12) Burroughs, A.; Kerenskaya, G.; Heaven, M. C. *J. Chem. Phys.* **2001**, *115*, 784.

(13) Schatz, G. C.; Gerber, R. B.; Ratner, M. A. *J. Chem. Phys.* **1988**, *88*, 3709.

(14) Garcıa-Vela, A.; Villarreal, P.; Delgado-Barrio, G. *J. Chem. Phys.* **1991**, *94*, 7868.

(15) Rubayo-Soneira, J.; Garcıa-Vela, A.; Villarreal, P.; Delgado-Barrio, G. *Chem. Phys. Lett.* **1995**, *243*, 236.

(16) Buchachenko, A. A. *Chem. Phys. Lett.* **1998**, *292*, 273.

(17) Garcıa-Vela, A. *J. Chem. Phys.* **1996**, *104*, 1047.

(18) An ab initio potential for the ground electronic state of I_2-Ar has been reported: Kunz, C. F.; Burghardt, I.; Hess, B. A. *J. Chem. Phys.* **1998**, *109*, 359.
(19) Gruebele, M.; Zewail, A. H. *J. Chem. Phys.* **1993**, *98*, 883.
(20) Note that there is a typesetting error in eq 17 of ref 19. In that paper the expression of q_1 reads $q_1 = 2.9343 \times 10^{-3}(D/Z)^2 p_0$ and should instead read $q_1 = 2.9343 \times 10^{-3}(D/Z^2)^{1/2} p_0$ (Zewail, A. H. Private communication).
(21) Aziz, R. A.; Slaman, M. J. *Chem. Phys.* **1989**, *130*, 187.
(22) Beswick, J. A.; Jortner, J. *Adv. Chem. Phys.* **1981**, *47*, Part I, 363.
(23) Gray, S. K.; Wozny, C. E. *J. Chem. Phys.* **1989**, *91*, 7671; **1991**, *94*, 2817.
(24) Engel, V. *Chem. Phys. Lett.* **1992**, *189*, 76.
(25) Ceotto, M.; Garcıa-Vela, A. *J. Chem. Phys.* **2001**, *115*, 2146.
(26) Tal-Ezer, H.; Kosloff, R. *J. Chem. Phys.* **1984**, *81*, 3967.
(27) Pernot, P.; Lester, W. A. *Int. J. Quantum Chem.* **1991**, *40*, 577.
(28) Le Quéré, F.; Gray, S. K. *J. Chem. Phys.* **1993**, *98*, 5396.
(29) Garcıa-Vela, A. *Chem. Phys. Lett.* **1998**, *290*, 155.